Assessing the accuracy of many-body expansions for the computation of solvatochromic shifts

Ricardo André Fernandes Mata

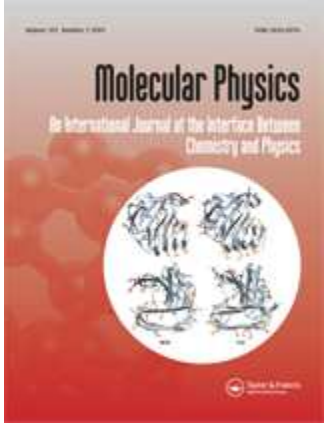

Assessing the accuracy of many-body expansions for the computation of solvatochromic shifts

Journal:	*Molecular Physics*
Manuscript ID:	TMPH-2009-0249.R1
Manuscript Type:	Special Issue Paper - In honour of Prof Werner 60th birthday
Date Submitted by the Author:	29-Oct-2009
Complete List of Authors:	Mata, Ricardo; Grupo de Física-Matemática da Universidade de Lisboa
Keywords:	many-body, spectra, solution, acetone, acrolein
Note: The following files were submitted by the author for peer review, but cannot be converted to PDF. You must view these files (e.g. movies) online.	
TMPH20090249R1.tar.gz	

Assessing the accuracy of many-body expansions for the computation of solvatochromic shifts

R. A. Mata

Grupo de Física-Matemática da Universidade de Lisboa,

Avenue Professor Gama Pinto 2, 1649-003 Lisboa, Portugal

Abstract

In this work, a computationally fast and simple scheme for calculating vertical excitation energies based on a many-body expansion is reviewed. It consists of a 2-body expansion where each of the energy terms is computed with embedding in a point charge field representing the environment. The neglect of 2-body polarization energy terms is evaluated, as it allows for a compact energy expression, and avoids parameterization of the solute. The solvatochromic shifts for the acetone and acrolein molecules are investigated, both in microsolvated clusters as well as in solution. It is found that the scheme is unable to correctly describe Rydberg states, but succeeds in closely reproducing the many-body effects involved in the $\pi \rightarrow \pi^*$ excitation of acrolein in water.

I. INTRODUCTION

The computational study of solvatochromic effects is still today a challenging task. On one hand, the theory should be able to accurately describe the electronic wavefunction (or density). This is opposed to the case of structural properties in solution, which can, to some extent, do without any explicit description of electrons through the use of molecular mechanics. On the other hand, one needs to describe a condensed phase or the effect thereof. This can be computationally demanding due to the size of the system and the conformational degrees of freedom involved. Some sort of compromise has to be found between the level of quantum mechanical treatment and the way the environment is included. One option is to treat the whole system explicitly, making use of an approximate model for the quantum treatment. Time-dependent density functional theory (TD-DFT)[1] has become increasingly popular over the last few years, as it allows for the computation of very large systems at a moderate cost. The level of accuracy is, however, strongly dependent of the system under treatment and the functional form chosen. Several deficiencies have been pointed out, and even doubts have been cast over the soundness of the approach[2–5]. Although this class of methods offers an improvement over semiempirical approaches which are still widely used, such as INDO/CIS[6], it is not obvious how the convergence of the results can be verified.

Another way around the problem is to approximate the environment effect, removing the solvent molecules from the quantum treatment. This is usually accomplished by means of hybrid quantum mechanics/molecular mechanics (QM/MM) calculations[7], and/or dielectric continuum models[8]. The first method has the advantage of treating solvent molecules explicitly, but this comes at a price, since conformational sampling is needed in order to obtain a description of the bulk. However, several methods have been proposed to reduce the computational cost involved in the sampling[9,10]. Both alternatives allow a significant reduction in the quantum system size without significantly affecting the accuracy. This, in turn, can be used to improve the electronic structure method in use. Nowadays, the most reliable ab initio approaches to the computation of spectra are based on coupled cluster theory. In particular, the response theory methods, including the CC2[11] and CC3[12] approximate models, and equation of motion variants such as coupled cluster with singles and double excitations (EOM-CCSD)[13]. Several applications have shown that the accuracy of these methods follows a well defined hierarchy CC2 < CCSD < CC3 < CCSDT < ....

However, even for the cheapest of all above mentioned methods (CC2), the computational cost scales with the fifth power relative to the system size, and this greatly limits the applicability to problems in solution. Some excitations require a delocalized description of the wavefunction over several solvent molecules and/or the use of large basis sets, which is not feasible with the conventional codes available. Local correlation versions of EOM-CCSD and CC2 (EOM-LCCSD[14] and LCC2[15]) have been presented in the last years, and offer a promising alternative. These are based on earlier work by Pulay and Saebø[16–18], and belong to an already long list of local correlation methods which have been successfully developed by Werner, Schütz and other coworkers[19–21]. These methods are today a reference in the field and have strongly pushed the community towards the development of faster and more accurate wavefunction methods.

A related approach to the problem, and which is straightforward to apply in the case of solvation problems, is the use of many-body expansions. Such approaches have been successfully applied for several years in determining the ground state energy of many different systems, from solid state[22–26] to molecular clusters[27–30], and even polypeptides[31,32]. Several alternatives have been formulated, either expanding the total energy or the correlation energy alone. The results have in general shown that the correlation energy can be computed very efficiently, even if the many-body expansion is truncated at two-body terms[33]. The HF or DFT energies can also be computed in a similar fashion, as long as an electrostatic embedding is used[28,29,34].

On the other hand, work on excited states has been scarce. Hirata *et al.*[27] computed the vertical excitation energy of formaldehyde in a large water cluster. Recently, Kitaura and coworkers[35,36] have applied their own fragment molecular orbital (FMO) approach to the computation of excitation spectra. The formaldehyde molecule in solution has also been studied under this approach[37].

The objectives of this work are twofold. First, the many-body formulation is revisited for the case of a solute and a solvent environment. By neglecting some of the expansion terms, an overall simple ansatz is obtained with reduced computational cost. The effect of this simplification is assessed. Secondly, there is still little information on the potential usefulness, or general applicability of this expansion. Most of the previous work has focused on applications where QM/MM approaches already work quite well (like the formaldehyde $n \rightarrow \pi^*$ excitation), or in systems where it is difficult to verify the results, either due to the

lack of experimental results or higher level quantum chemical data. Therefore, two different molecular systems will be studied, comparing the effects of the expansion for smaller clusters (using high-level benchmark results) and for the system in condensed phase (by comparing with experimental data).

II. METHOD

In this Section, the nomenclature found in the work of Chiba *et al.*[35] is used. One starts by expanding the energy of the system in a many-body formulation. In this work, each calculation will be performed in the point charge field of the neighboring molecules. This leads to a faster convergence in the expansion, since it introduces approximate N-body Coulombic effects. If we consider a system composed of a solute molecule M in its excited state, and the remaining solvent molecules in their ground state, the energy expression up to two-body terms is given by

$$E^* = E^*_M + \sum_{I\neq M} E^{0'}_I + \sum_{I\neq M} \left(E^*_{MI} - E^*_M - E^{0'}_I\right) + \sum_{\substack{I<J \\ I,J\neq M}} \left(E^{0'}_{IJ} - E^{0'}_I - E^{0'}_J\right), \tag{1}$$

where I and J are indices for the solvent molecules, the superscripts $*$ and 0 stand for excited and ground states, respectively, and the apostrophe signals the fact that the solvent molecules experience a solute charge corresponding to M in the excited state. In order to compute the value of E^*, one has to determine the solvent charges, the solute (ground and excited state) charges, and run a calculation for each monomer and dimer with a point charge field representing the environment.

To calculate the excitation energy, one needs to define the ground state energy, which is given by

$$E^0 = E^0_M + \sum_{I\neq M} E^0_I + \sum_{I\neq M} \left(E^0_{MI} - E^0_M - E^0_I\right) + \sum_{\substack{I<J \\ I,J\neq M}} \left(E^0_{IJ} - E^0_I - E^0_J\right), \tag{2}$$

the only differences being that the energy terms involving the solute are computed for the ground state, and that the embedding field used for the solvent molecules represents

the charge distribution of the ground state solute. One should note that these equations consider a non-polarizable model for the charges.

If one introduces the approximation that the charge distribution change in the solute has a negligible effect on the solvent energy terms ($E_I^{0'} \simeq E_I^0$ and $E_{IJ}^{0'} \simeq E_{IJ}^0$), the excitation energy reduces to a very simple expression

$$\omega_{\mathrm{R2B}} = E_M^* - E_M^0 + \sum_{I \neq M} \left(E_{MI}^* - E_{MI}^0 + E_M^0 - E_M^* \right), \tag{3}$$

which includes only solute terms and a single sum over the solvent molecules. This value will be refered to as a reduced two-body vertical transition energy (R2B-VTE). The difference between the full 2-body expression and Eq. (3) is given by

$$\omega_{\mathrm{2B}} - \omega_{\mathrm{R2B}} = \sum_{\substack{I<J \\ I,J \neq M}} \left(E_{IJ}^{0'} - E_{IJ}^0 + E_I^0 - E_I^{0'} + E_J^0 - E_J^{0'} \right). \tag{4}$$

In order to better understand this result, we now consider a two-body expansion of the solvent polarization energy (due to the solute excitation)

$$P_{\mathrm{solv}} = \sum_{I \neq M} P_I + \sum_{\substack{I<J \\ I,J \neq M}} \left(P_{IJ} - P_I - P_J \right) \tag{5}$$

$$P_I = E_I^{0'} - E_I^0 \tag{6}$$

$$P_{IJ} = E_{IJ}^{0'} - E_{IJ}^0. \tag{7}$$

Comparing Eqs. (4) and (5), it is clear that the difference between the full 2-body result and R2B-VTE is the 2-body solvent polarization energy. This reflects the change in the interaction energy between two solvent molecules, due to the change in the solute charge distribution. The one-body effect is already contained in the result of Eq. (3) through the difference $E_{MI}^* - E_{MI}^0$. Since these terms dominate the expansion, as it should converge rather quickly, the difference is expected to be quite small. On a side note, truncating the series at the 1-body level, and applying the same approximation (R1B-VTE), one is left with the first term in Eq. (1) which is a QM/MM electrostatic embedding result[38]. Excitonic coupling could also be included just as in Ref. 39, but in this work only single chromophores will be considered.

The advantages of Eq. (3) are manifold. Firstly, if one considers the computational cost of including the point charges in the Hamiltonian to be negligible, the calculation cost will

scale linearly with the number of solvent molecules. Secondly, one never needs to define a point charge distribution for the solute, since all energy terms include the molecule in the quantum system. The only parameter one has to define is the solvent charge distribution. The limitation of this method, such as any other many-body based formulation, is that the excitation under study should be energetically separated from the solvent spectra in order to correctly single it out in the dimer calculations. This expression has been formerly used in the context of FMO and in another simplified many-body study[27]. In the latter, the embedding was performed with the use of dipoles for each solvent molecule. The effect of the 2-body polarization terms (Eq. (4)) has been, however, not discussed.

The acetone (Act) and acrolein (Acr) molecules were the chosen test subjects for this work. In particular, the first two excitation energies of each species. In both cases, the first absorption in the monomer corresponds to a $n \rightarrow \pi^*$ excitation. It will be interesting to compare the errors and verify the stability of the approach relative to changes in the molecular species. The second excitation in acetone is a $n \rightarrow 3s$ Rydberg type excitation. This is the first in a set of Rydberg excitations, but is well separated from the remaining[40,41], both in the gas and in solution. In order to correctly describe the Rydberg state, large and diffuse basis sets are needed. This can become a problem when applying many-body approximations, since the contribution of higher terms (in this case, only two-body contributions) may be overestimated, as they can compensate for basis set incompleteness effects (BSIE) in the monomer or, reversely, lacking higher-order basis contributions. It is questionable whether this type of expansions can be safely used in such cases. Finally, the last excitation in acrolein, which is of the $\pi \rightarrow \pi^*$ type. This carries other computational challenges, namely in solution. It is known that the solvatochromic shift is strongly dependent of the number of water molecules included in the quantum mechanical calculation[42].

III. RESULTS AND DISCUSSION

A. Gas Results

We start by examining results for the molecules *in vacuo*. The acetone and acrolein geometries were optimized at the MP2/aug-cc-pVTZ level of theory (see Supplementary Information). Both structures were found to be in general good agreement with the exper-

imental data of Refs. 43 and 44,45, respectively. In the case of acrolein, the most relevant difference is perhaps a slight overestimation of the C=O double bond length. The $n \rightarrow \pi^*$ excitation energy, just as in the case of acetone[46], is rather sensitive to this value[42].

In order to study the basis set dependence, the excitation energies were computed using the MP2-optimized monomer geometries. EOM-CCSD[47] was the computational method chosen, and the basis sets included were the Dunning aug-cc-pVXZ (X=D,T,Q)[48] and the respective double-augmented d-aug-cc-pVXZ (X=D,T) sets[49]. The results are shown in Table I.

The acrolein $n \rightarrow \pi^*$ and $\pi \rightarrow \pi^*$ excitations seem to be well converged even at the EOM-CCSD/aug-cc-pVDZ level. Comparing to the largest basis sets in this study (d-aug-cc-pVTZ and aug-cc-pVQZ), the excitation energies change only by about 0.02 eV. The same is observed for the $n \rightarrow \pi^*$ excitation of acetone. The $n \rightarrow 3s$ excitation, however, exhibits a completely different behavior. Even with the largest basis sets it is difficult to confirm whether the excitation energy is converged. This is of course linked to the fact that this a Rydberg-type excitation, where the excited electron has a very diffuse density. In any case, the most significant improvement occurs on changing from double- to triple-ζ, and the aug-cc-pVTZ value can be considered to be at least qualitatively reasonable. Comparing to the experimental estimates, the $n \rightarrow \pi^*$ values agree to within 0.2 eV, which is more or less expected from the method. The best comparison is in the case of acetone, which is probably linked to the better agreement between the optimized MP2 C=O distance and the experimental estimate. The error in the acetone $n \rightarrow 3s$ excitation is somewhat larger, with the best estimate (EOM-CCSD/aug-cc-pVQZ) overshooting by about 0.3 eV. The worst comparison is in the acrolein $\pi \rightarrow \pi^*$ case, with errors above 0.4 eV. The reason behind this discrepancy may be linked to the geometry, or even the approximations made in comparing to the experimental estimate. A more thorough discussion of this subject can be found in Ref. 42 and references therein. The fact that the EOM-CCSD errors are of the same order of magnitude as the expected solvatochromic shifts should be taken into consideration. It is a further evidence for the difficulties found in computing this quantity. Even at a such high-level of theory one has to rely on error compensation in comparing the gas phase excitation to the one in solution. Any approximation should be robust enough to keep the errors constant in both cases.

B. Cromophore-water clusters

In this Section, results are presented for test calculations on small clusters containing water and the two molecules under study (acetone and acrolein). The $\mathrm{Act}(\mathrm{H_2O})_N$ and $\mathrm{Acr}(\mathrm{H_2O})_N$ ($N = 1 - 5$) structures were optimized at the DF-LMP2/cc-pVTZ level[50,51]. A Boughton-Pulay criteria[52] of 0.985 was used throughout. They compare well with the MP2 optimized geometries (see Supplementary Information). In order to consistently study the excitation shift, the monomer geometry was reoptimized at the same level of theory. The cluster structures are shown in Figs. 1 and 2. The structures were generated by manually placing water molecules around each solute and reoptimizing at the same level. No claim is made as to whether these include the global minima. However, one should note that the goal is to simply sample some relevant coordination sites on each molecule. In the case of acetone, both excitations are mainly located in the carbonyl moiety, and water molecules were accordingly placed close to this fragment. In the case of acrolein, the effect of water molecules close to the C=C double bond should also be relevant and, therefore, structures were generated where water is only loosely bound to the hydrophobic section of acrolein. Although energetically unfavorable, such clusters are relevant to the present study. These calculations were performed with the `Molpro` 2008.1 program package[53].

Taking into account the results of Table I, and in order to benchmark clusters with a significant number of water molecules, the smallest basis set (aug-cc-pVDZ) was used. The basis set is clearly too small for the Act $n \rightarrow 3s$ case, but since one is mostly interested in excitation energy shifts, some error compensation should be expected. Three sets of calculations were performed for each structure. The EOM-CCSD/aug-cc-pVDZ excitation energies were computed with no approximations, with a full 2-body treatment (2B-VTE), and the reduced 2-body expression (R2B-VTE). The charges used for describing the water molecules were taken from the TIP3P potential[54]. In order to compute the 2B-VTE, one also needs to define ground and excited states charges for the solute. For this purpose, the Mulliken charges[55] of the monomer for the ground and excited states were taken from the HF/aug-cc-PVTZ and the CIS/aug-cc-PVTZ solutions, respectively. The many-body calculations were automated through in-house Python scripts interfaced to Molpro[34].

The results are shown in Tables II and III. The full 2-body results are not given. Instead, the difference between the full and the reduced expression (which ammounts to the 2-body

polarization) is shown. For more detailed information, the reduced 1-body result (R1B-VTE or QM/MM) is also given.

We start by examining the results for the acetone molecule (Table II). The first excitation values for the full calculation and R2B-VTE agree extremely well. The maximum deviation is 0.015 eV, but the errors are mostly below 0.007 eV. This is just a small improvement relative to the R1B-VTE (QM/MM) result. The maximum deviation for the latter is 0.027 eV, and the average errors are also about double of the 2-body result. Since both errors are small, particularly compared to the EOM-CCSD errors, the gain in accuracy is not particularly relevant. The 2-body polarization contribution, which should be added to the R2B-VTE in order to obtain the full 2-body result, is found to be small. It would, however, lead to an overestimation of the excitation energies. The reduced expansion is more accurate than the full 2B-VTE result. This is certainly linked to the use of population analysis to define the solute charges.

The $n \rightarrow 3s$ excitation values show a somewhat different pattern. Although one does observe a general improvement of the R2B-VTE set relative to the one-body energies, there are some cases where the results are in fact worsened. The overall picture is that the 2-body correction leads to no systematic improvement. This places doubts on the robustness of the method, and the convergence of the many-body expansion for this excitation. The R2B-VTE values tend to underestimate the shift. In order to better study this effect, the calculations for $\mathrm{Act(H_2O)}_N$ for $N \leq 3$ were repeated with the aug-cc-pVTZ basis set. The errors between the full EOM-CCSD calculation and the R2B-VTE and R1B-VTE values for the two basis sets (aug-cc-pVDZ and aug-cc-pVTZ) were computed. The results are displayed in Fig. 3.

As pointed above, using the aug-cc-pVDZ basis, a systematic convergence pattern is not observed. For structure act3A, the R1B-VTE has an even smaller error than the 2-body result. But even with the aug-cc-pVTZ basis, little to no improvement is observed. Although the results for the smaller structures show a better convergence, when three water molecules are included, the 2-body results fail in improving over the 1-body values. Therefore, the errors in the expansion seem to be inherent to the approach, and not simply due to the particular basis set in use (aug-cc-pVDZ). Although the differences are still rather small (relative to full EOM-CCSD), they may accumulate for larger systems. This effect is further studied in the next Section.

The results for acrolein clusters are shown in Table III. The discussion of the acetone $n \rightarrow \pi^*$ excitation is easily extended to the acrolein case. The R2B-VTE set is in excellent agreement with the full results, the many-body expansion being seemingly converged. The largest difference between the two cases is that the errors at the one-body level are somewhat higher, and that the predicted 2-body polarization contribution is significantly smaller. However, just as for acetone, adding these terms would lead to no improvement. The results for $\pi \rightarrow \pi^*$ are, as expected, the ones which more clearly show the benefits of including two-body terms. As previously discussed, to correctly describe this excitation, one needs to include a relatively large number of water molecules in the quantum calculation. The R2B-VTE errors are close to the ones observed for the first excitation. The one-body values, however, deviate up to 0.08 eV, the largest errors found in the test set. It should be noted that this deviation is still relatively small. However, based on the conclusions of Aidas et al.[42], we can expect that the error will continue to accumulate on going to larger systems. This is not possible to verify by comparing to full calculations since the $Acr(H_2O)_5$ system size is close to the computational limit. However, these calculations on the smaller systems already give useful indications for the study in aqueous solution, which is developed in the next Section.

C. Solvatochromic shifts

The electronic excitation spectra of acrolein and acetone in solution have been the subject of several theoretical works. In the case of acrolein, results are available for both the $n \rightarrow \pi^*$ solvatochromic shift[42,56–63] as well as the $\pi \rightarrow \pi^*$ shift[42,56,58,59]. The $n \rightarrow \pi^*$ experimental estimate (0.19-0.21 eV)[64–66] is in the most recent studies systematically reproduced. The most challenging quantity is the $\pi \rightarrow \pi^*$ shift, which appears to have a large dependence on the quantum system size. QM/MM results, including only the acrolein in the quantum system, underestimate the value by more than 50%[42,58]. This effect was already visible in the cluster results (Table III), and it will be interesting to observe the impact of the 2-body contributions in solution.

The acetone $n \rightarrow \pi^*$ solvatochromic shift has also deserved considerable attention[46,57,67–81]. Less is known about the Rydberg states, as well as other higher excitations. This is partly due to difficulties in describing state coupling at higher energies

(between $3p$ Rydberg and π^* states)[40]. Another reported problem in the study of acetone is the existence of spurious solute to solvent charge transfer excitations when using TD-DFT[76]. This is yet another argument for the development of faster and more robust *ab initio* approaches to the study of excitation spectra in solution.

In order to calculate the solvatochromic shifts of both molecules in water solution, a molecular dynamics (MD) simulation was carried out for each. The gas phase geometries were reoptimized at the same level (MP2/aug-cc-pVTZ), but with a polarizable continuum model (PCM)[8] replicating the effect of a water environment ($\epsilon = 78.39$). The PCM calculations were carried out with the Gaussian03 program package[82]. The two monomer structures were then placed in the center of a pre-equilibrated cubic box of TIP3P water molecules[54], with an edge length of 24.846 Å. Superimposing water molecules were removed. The molecular mechanics potential terms for acetone were taken from the OPLS potential[83], for acrolein the same potential as in Ref. 42 was used. The system was equilibrated with 200,000 steps of NVT rigid-body dynamics (T=298.15 K), with a time-step of 1 fs. A vdW cutoff of half the box size was used, and an Ewald sum for the electrostatics (with a cutoff of 9.0 Å, and a reciprocal space fraction of 0.35 in the reciprocal sum). After equilibration, the same step size was used for a 1.0 ns production run. System preparation and all molecular mechanics calculations were carried out using the TINKER suite of programs[84]. For each snapshot, a sphere centered on the oxygen atom (of each molecule) and including all water molecules up to a distance of 20 Å was cut from the total system. This includes some replica water molecules.

In order to compute the solvatochromic shift, the R2B-VTE expression was used, but including only a limited number of waters in the quantum system. One could, in principle, use the whole sphere in the calculation, but due to the system size, this is not practical. The embedding field includes all waters in the sphere, but dimer corrections are only computed up to a number n_w of solvent molecules. For each of the excitations, the convergence of the solvatochromic shift relative to n_w has been analyzed. The water molecules were ordered in both cases according to the distance to the carbon of the carbonyl moiety. The excitation energies were computed at the EOM-CCSD/aug-cc-pVDZ level of theory, except for the $n \rightarrow 3s$ acetone excitation, where the aug-cc-pVTZ basis was also used. The solvatochromic shift is defined as the energy difference between the excitation energy of the MP2(PCM)/aug-cc-pVTZ optimized structure, dipped in the solvent box, and of the gas phase MP2/aug-

cc-pVTZ optimized molecule. Results for different quantum sizes (n_w) are given in Figs. 4 (acetone) and 5 (acrolein). It should be noted that by including n_w water molecules in the calculation, the result for any given subgroup is also directly extracted, due to the incremental procedure used. This is another important advantage of this approach, as it allows to check for convergence in the quantum system size. The final data is also compiled in Table IV, including the experimental estimates for comparison.

In the case of acetone, the convergence with n_w is remarkably good, with the QM/MM value ($n_w = 0$) already providing a reasonable estimate on the solvent effect. Two regimes are distinguishable. For smaller n_w values, there is a larger dependence, which is certainly due to the inclusion of quantum effects, such as exchange or electronic correlation. Above $n_w = 20$, the $\Delta\omega$ value slowly changes with increasing number of water molecules, but the shift is only of about 0.007 eV up to $n_w = 50$. This second regime could be probably linked to an improved description of the electrostatic field (over the TIP3P point charges). The $n \rightarrow \pi^*$ shift for $n_w = 50$ (0.115 ± 0.015) deviates somewhat from the measured experimental shift. However, it is found to be in good agreement with previous theoretical estimates, which also underestimate the solvatochromic effect (see Ref. 46 and references therein). This discrepancy is not necessarily linked to the many-body scheme. The difference is still rather small (around 0.08 eV), and could also be due to the underlying quantum chemical method (EOM-CCSD).

The solvatochromic shift of the $n \rightarrow 3s$ excitation, contrary to the $n \rightarrow \pi^*$ case, shows no convergence pattern. The values of $\Delta\omega$ show a linear dependence relative to n_w. Increasing the basis set also leads to no visible improvement. Calculations up to $n_w = 12$ were performed with the aug-cc-pVTZ and d-aug-cc-pVDZ basis (the former values are also shown in Figure 4). The dependence on n_w shows a very similar pattern in all cases. There is a first regime where the excitation energy rises ($n_w < 5$), and a second regime, when including water molecules which are further away from the solute, where the shift is lowered. The first effect can be easily accounted for. Due to the diffuse character of the excitation, it is expectable that some of the excited state electronic density will overlap with the surrounding charges. This leads to errors in the one-body term, since the point charge approximation is inadequate for such cases. By advancing to two-body terms, quantum effects between the solute and solvent densities are included, and the excited state energy increases. The positive point charges which represent the neighbouring water hydrogens are replaced by an

explicit electronic description, and this effect destabilizes the excited state. These corrections should be additive. At larger distances, a second effect comes into play. By adding a distant quantum water molecule and the respective basis functions, the excited electron is able to localize in regions of space away from the solute. Even if one significantly increases the basis set, the basis functions are still centered on the chromophore, and do not allow for a full charge delocalization. This effect is not additive and leads to the breakdown of the many-body approximation. Possible solutions to this problem would be the use of a non-local basis (such as plane waves, or a mixed basis set), a more realistic embedding environment (pseudopotentials) or even applying constraints to the excitation. The $n \rightarrow 3s$ shift has been excluded from Table IV since no reliable estimate is available.

The results for the $n \rightarrow \pi^*$ excitation of acrolein, just as in the case of acetone, are quickly converged. The estimate of 0.240 ± 0.022, obtained as an average over 20 configurations, agrees well with the experimental value. As in the $n \rightarrow \pi^*$ excitation of acetone, above $n_w = 20$ the values change only slightly. The shift for the $\pi \rightarrow \pi^*$ shows, however, a different behavior. In agreement with the observations of Aidas *et al.*[42], a very large quantum system is needed. Their maximum quantum system included 12 water molecules, with shifts of -0.43 (TIP3P embedding) and -0.46 eV (SPCpol embedding) at the CAM-B3LYP level of theory. Due to the many-body expansion, it is simple in this case to expand even further the quantum system and, in fact, confirm that above $n_w = 12$ the shift is still further to the red. The effect is so pronounced, that the $n_w = 0$ shift is less than half of that obtained with $n_w = 50$. The R2B-VTE estimate (-0.558 ± 0.032 eV) is in much closer agreement with the experimental result of -0.52 eV.

The estimates presented in Table IV, although computed at a relatively high-level of theory and with explicit treatment of solvent quantum effects, have been extracted from a relatively small sampling set (20 MD snapshots). The statistical errors associated are around 10% of the total solvatochromic shift. This could be improved by a more thorough sampling procedure. However, the main purpose of this work was not so much to obtain converged values for the excitations, but to observe the effect of the many-body expansion on the shifts. The main conclusions should not be affected by this fact.

IV. CONCLUSIONS

The use of many-body expansions for the computation of solvatochromic shifts has been reviewed. From the test set used, the solvatochromic shift of the $\pi \rightarrow \pi^*$ acrolein excitation is the case where this approach proved of greater usefulness, successfully capturing the effect of the environment and improving the computational estimate. A strong dependency on the quantum system size has also been observed for similar valence excitations in other molecules, such as in the uracyl molecule[85]. The many-body expansion here reviewed could help to elucidate this effect. One of the major benefits of the method is that the reference wavefunction is also computed in an incremental fashion, removing one further computational bottleneck. For the $n \rightarrow \pi^*$ excitations, the value is only marginally affected by the 2-body contributions, with the QM/MM estimates delivering reasonable results. The acetone $n \rightarrow 3s$ case, the only Rydberg state under study in this work, is seen to be inadequately described by this scheme. Although in the smaller clusters the R2B-VTE can improve on the one-body result, this is found to be inconsistent, even when applying a larger local basis.

One of the questions placed in this work was regarding the neglect of 2-body polarization terms, which allows for a reduced energy expression. These terms are found to have an overall negligible effect under the expansion used in this work. In some cases, and due to the approximative nature of the terms, it does even affect the quality of the results.

A question which has not been addressed in this work is the combination of different quantum chemical methods in the scheme. In principle, it should be possible to apply a high level (and computationally more expensive) method for the calculation of the 1B-VTE, and a lower level approach for the 2-body increments. This is the same philosophy behind the local pair approximations of Werner and coworkers[19,21,86]. However, the lower level method will still have to include dynamic correlation effects. The best foreseeable approach would be to combine CC3 or CCSD with the lower CC2 level of theory. Improvements in this line are being currently pursued.

V. ACKNOWLEDGEMENTS

Financial support from the Fundação para a Ciência e Tecnologia (grant reference SFRH/BPD/38447/2007) is gratefully acknowledged.

---

[1] M. A. L. Marques and E. K. U. Gross, Annu. Rev. Phys. Chem. **55**, 427 (2004).

[2] J. Schirmer and A. Dreuw, Phys. Rev. A **75**, 022513 (2007).

[3] N. T. Maitra, , R. van Leeuwen, and K. Burke, Phys. Rev. A **78**, 056501 (2008).

[4] J. Schirmer and A. Dreuw, Phys. Rev. A **78**, 056502 (2008).

[5] A. Holas, M. Cinal, and N. H. March, Phys. Rev. A **78**, 016501 (2008).

[6] J. Ridley and M. C. Zerner, Theor. Chim. Acta **32**, 111 (1973).

[7] A. Warshel and M. Levitt, J. Mol. Biol. **103**, 227 (1976).

[8] J. Tomasi, B. Mennucci, and R. Cammi, Chem. Rev. **105**, 2999 (2005).

[9] K. Coutinho, S. Canuto, and M. C. Zerner, J. Chem. Phys. **66**, 249 (2000).

[10] M. E. Martín, M. L. Sánchez, F. J. O. D. Valle, and M. A. Aguilar, J. Chem. Phys. **113**, 6308 (2000).

[11] O. Christiansen, H. Koch, and P. Jørgensen, Chem. Phys. Lett. **243**, 409 (1995).

[12] O. Christiansen, H. Koch, and P. Jørgensen, J. Chem. Phys. **103**, 7429 (1995).

[13] J. Geertsen, M. Rittby, and R. J. Bartlett, Chem. Phys. Lett. **164**, 57 (1989).

[14] T. Korona and H.-J. Werner, J. Chem. Phys. p. 3006 (2003).

[15] D. Kats, T. Korona, and M. Schütz, J. Chem. Phys. **127**, 064107 (2007).

[16] P. Pulay, Chem. Phys. Lett. **100**, 151 (1983).

[17] S. Saebø and P. Pulay, Chem. Phys. Lett. **113**, 13 (1985).

[18] S. Saebø and P. Pulay, Annu. Rev. Phys. Chem. **44**, 213 (1993).

[19] C. Hampel and H.-J. Werner, J. Chem. Phys. **104**, 6286 (1996).

[20] M. Schütz, G. Hetzer, and H.-J. Werner, J. Chem. Phys. **111**, 5691 (1999).

[21] M. Schütz and H.-J. Werner, J. Chem. Phys. **114**, 661 (2001).

[22] H. Stoll, Chem. Phys. Lett. **191**, 548 (1992).

[23] H. Stoll, Phys. Rev. B **46**, 6700 (1992).

[24] R. Pardon, J. Gräfenstein, and G. Stollhoff, Phys. Rev. B **51**, 10556 (1995).

[25] K. Doll, M. Dolg, P. Fulde, and H. Stoll, Phys. Rev. B **52**, 4842 (1995).

[26] B. Paulus, P. Fulde, and H. Stoll, Phys. Rev. B **54**, 2556 (1996).

[27] S. Hirata, M. Valiev, M. Dupuis, S. S. Xantheas, S. Sugiki, and H. Sekino, Mol. Phys. **103**, 2255 (2005).

[28] E. E. Dahlke and D. G. Truhlar, J. Chem. Theory and Comp. **3**, 46 (2007).

[29] M. Kamiya, S. Hirata, and M. Valiev, J. Chem. Phys. **128**, 074103 (2008).

[30] K. Kitaura, T. Sawai, T. Asada, T. Nakano, and M. Uebayasi, Chem. Phys. Lett. **312**, 319 (1999).

[31] K. Kitaura, E. Ikeo, T. Asada, T. Nakano, and M. Uebayasi, Chem. Phys. Lett. **313**, 701 (1999).

[32] T. Nakano, T. Kaminuma, T. Sato, K. Fukuzawa, Y. Akiyama, M. Uebayasi, and K. Kitaura, Chem. Phys. Lett. **351**, 475 (2002).

[33] J. Friedrich, M. Hanrath, and M. Dolg, J. Chem. Phys. **126**, 154110 (2007).

[34] R. A. Mata and H. Stoll, Chem. Phys. Lett. **465**, 136 (2008).

[35] M. Chiba, D. G. Fedorov, and K. Kitaura, J. Chem. Phys. **127**, 104108 (2007).

[36] H. Fukunaga, D. G. Fedorov, M. Chiba, K. Nii, and K. Kitaura, J. Phys. Chem. A **112**, 10887 (2008).

[37] Y. Mochizuki, Y. Komeji, T. Ishikawa, T. Nakano, and H. Yamataka, Chem. Phys. Lett. **437**, 66 (2007).

[38] H. M. Senn and W. Thiel, Top. Curr. Chem. **268**, 173 (2007).

[39] R. A. Mata, H. Stoll, and B. J. C. Cabral, J. Chem. Theory and Comp. **5**, 1829 (2009).

[40] B. Hess, P. J. Bruna, R. J. Buenker, and S. D. Peyerimhoff, Chem. Phys. **18**, 267 (1976).

[41] M. Mérchan, B. O. Roos, R. McDIarmid, and X. Xing, J. Chem. Phys. **104**, 1791 (1996).

[42] K. Aidas, A. Møgelhøj, E. J. K. Nilsson, M. S. Johnson, K. V. Mikkelsen, O. Christiansen, P. Söderhjelm, and J. Kongsted, J. Chem. Phys. **128**, 194503 (2008).

[43] L. M. Sverdlov, M. A. Kovner, and E. P. Krainov, *Vibrational Spectra of Polyatomic Molecules* (Wiley, New York, 1974).

[44] E. A. Cherniak and C. C. Costain, J. Phys. Chem. **45**, 104 (1966).

[45] C. E. Blom, G. Grassi, and A. Bauder, J. Am. Chem. Soc. **106**, 7427 (1984).

[46] K. Aidas, J. Kongsted, A. Osted, K. V. Mikkelsen, and O. Christiansen, J. Phys. Chem. A **109**, 8001 (2005).

[47] J. F. Stanton and R. J. Bartlett, J. Chem. Phys. **98**, 7029 (1993).

[48] R. A. Kendall, T. H. Dunning, and R. J. Harrison, J. Chem. Phys. **96**, 6796 (1992).

[49] D. E. Woon and T. H. D. Jr., J. Chem. Phys. **100**, 2975 (1994).

[50] H.-J. Werner, F. R. Manby, and P. Knowles, J. Chem. Phys. **118**, 8149 (2003).

[51] M. Schütz, H.-J. Werner, R. Lindh, and F. R. Manby, J. Chem. Phys. **121**, 737 (2004).

[52] J. W. Boughton and P. Pulay, J. Comput. Chem. **14**, 736 (1993).

[53] H.-J. Werner, P. J. Knowles, R. Lindh, F. R. Manby, M. Schütz, et al., *Molpro, version 2008.1, a package of ab initio programs* (2008), see http://www.molpro.net.

[54] W. L. Jorgensen, J. Chandrasekhar, J. D. Madura, R. W. Impey, and M. L. Klein, J. Chem. Phys. **79**, 926 (1983).

[55] R. S. Mulliken, J. Chem. Phys. **23**, 1833 (1955).

[56] S. Iwata and K. Morokuma, J. Am. Chem. Soc. **97**, 966 (1975).

[57] S. Ten-no, F. Hirata, and S. J. Kato, J. Chem. Phys. **100**, 7443 (1994).

[58] F. Aquilante, V. Barone, and B. O. Roos, J. Chem. Phys. **119**, 12323 (2003).

[59] S. A. do Monte, T. Müller, M. Dallos, H. Lischka, M. Diedenhofen, and A. Klamt, Theor. Chim. Acta **111**, 78 (2004).

[60] M. E. Martín, A. M. Losa, I. Fdez.-Galán, and M. A. Aguilar, J. Chem. Phys. **121**, 3710 (2004).

[61] H. C. Georg, K. Coutinho, and S. Canuto, J. Chem. Phys. **123**, 124307 (2005).

[62] G. Brancato, N. Rega, and V. Barone, J. Chem. Phys. **125**, 164515 (2006).

[63] A. M. Losa, I. Fdez.-Galván, M. A. Aguilar, and M. E. Martín, J. Phys. Chem. B **111**, 9864 (2007).

[64] N. S. Bayliss and E. G. McRae, J. Chem. Phys. **58**, 1006 (1954).

[65] W. P. Hayes and C. J. Timmons, J. Spectrochim. Acta **21**, 529 (1965).

[66] N. S. Bayliss and G. Wills-Johnson, Spectrochim. Acta, Part A **24**, 551 (1968).

[67] J. Gao, J. Am. Chem. Soc. **116**, 9324 (1994).

[68] L. Serrano-Andrés, M. P. Fülscher, and G. Karlström, Int. J. Quantum Chem. **65**, 167 (1997).

[69] D. W. Liao, A. M. Mebel, Y. T. Chen, and S. H. Lin, J. Phys. Chem. A **65**, 167 (1997).

[70] K. Coutinho, N. Saavedra, and S. Canuto, J. Mol. Struct. THEOCHEM **466**, 69 (1999).

[71] F. C. Grozema and T. P. van Duijnen, J. Phys. Chem. A **102**, 7984 (1998).

[72] M. Cossi and V. Barone, J. Chem. Phys. **112**, 2427 (2000).

[73] F. Aquilante, M. Cossi, O. Crescenzi, G. Scalmani, and V. Barone, Mol. Phys. **101**, 1945 (2003).

[74] U. F. Röhrig, I. Frank, J. Hutter, A. Laio, J. VandeVondele, and U. Rothlisberger,

ChemPhysChem **4**, 1177 (2003).

[75] K. Coutinho and S. Canuto, J. Mol. Struct. THEOCHEM **632**, 235 (2003).

[76] L. Bernasconi, M. Sprik, and J. Hutter, J. Chem. Phys. **119**, 12417 (2003).

[77] O. Crescenzi, M. Pavone, F. D. Angelis, and V. Barone, J. Phys. Chem. B **109**, 445 (2005).

[78] M. Pavone, G. Brancato, G. Morelli, and V. Barone, ChemPhysChem **7**, 148 (2006).

[79] H. C. Georg, K. Coutinho, and S. Canuto, Chem. Phys. Lett. **429**, 119 (2006).

[80] A. Öhrn and G. Karlström, Theor. Chim. Acta **117**, 441 (2007).

[81] S. Hoyau, N. B. Amor, S. Borini, S. Evangelisti, and D. Maynau, Chem. Phys. Lett. **451**, 141 (2008).

[82] M. J. Frisch, G. W. Trucks, H. B. Schlegel, G. E. Scuseria, M. A. Robb, J. R. Cheeseman, J. A. Montgomery, T. Vreven, K. N. Kudin, J. C. Burant, et al., *Gaussian 03, revision c.02* (2003).

[83] W. L. Jorgensen, D. S. Maxwell, and J. Tirado-Rives, J. Am. Chem. Soc. **117**, 11225 (1996).

[84] J. W. Ponder, *TINKER: Software Tools for Molecular Design; 4.2 ed.* (Washington University School of Medicine: Saint Louis, 2003).

[85] V. Ludwig, K. Coutinho, and S. Canuto, Phys. Chem. Chem. Phys. **9**, 4907 (2007).

[86] G. Hetzer, M. Schütz, H. Stoll, and H.-J. Werner, J. Chem. Phys. **113**, 9443 (2000).

[87] W. M. S. J. III, R. C. Estler, and J. P. Doering, J. Chem. Phys. **61**, 763 (1974).

[88] J. G. Philis and L. Goodman, J. Chem. Phys. **98**, 3795 (1993).

[89] F. E. Blacet, W. G. Young, and J. G. Roof, J. Am. Chem. Soc. **59**, 608 (1937).

[90] J. M. Hollas, Spectrochim. Acta **19**, 1425 (1963).

[91] A. F. Moskvin, O. P. Yablonkii, and L. F. Bondar, Theor. Exp. Chem. **2**, 636 (1966).

Tables

Table I: Vertical excitation energies (in eV) for the molecules under study. The geometries have been optimized at the MP2/aug-cc-pVTZ level, the excitation energies have been computed with the EOM-CCSD method.

Acetone

	$n \rightarrow \pi^*$	$n \rightarrow 3s$
aug-cc-pVDZ	4.494	6.401
d-aug-cc-pVDZ	4.487	6.371
aug-cc-pVTZ	4.502	6.591
d-aug-cc-pVTZ	4.500	6.572
aug-cc-pVQZ	4.518	6.659
Experiment	4.38-4.49[a]	6.35[b]

Acrolein

	$n \rightarrow \pi^*$	$\pi \rightarrow \pi^*$
aug-cc-pVDZ	3.880	6.845
d-aug-cc-pVDZ	3.875	6.830
aug-cc-pVTZ	3.886	6.849
d-aug-cc-pVTZ	3.884	6.845
aug-cc-pVQZ	3.901	6.850
Experiment	3.69[c]	6.42[d]

[a]- Refs. 42,64,87.

[b] - Ref. 88.

[c] - Refs. 89,90.

[d] - Ref. 91.

Table II: Excitation energies (in eV) for acetone-water clusters together with a decomposition of the many-body contributions. The geometries have been optimized at the DF-LMP2/cc-pVTZ level, the excitation energies have been computed with EOM-CCSD/aug-cc-pVDZ.

		$n \rightarrow \pi^*$				$n \rightarrow 3s$			
Structure	Tag	FULL	R2B-VTE[a]	R1B-VTE[b]	2B-Pol[c]	FULL	R2B-VTE[a]	R1B-VTE[b]	2B-Pol[c]
Act		4.503				6.406			
$Act(H_2O)_1$	act1A	4.633	4.633	4.643	—	6.742	6.742	6.736	—
$Act(H_2O)_2$	act2A	4.752	4.750	4.770	0.001	7.042	7.029	7.030	0.000
	act2B	4.665	4.667	4.669	0.007	6.909	6.910	6.899	0.001
	act2C	4.682	4.675	4.677	0.023	6.814	6.800	6.760	0.004
$Act(H_2O)_3$	act3A	4.650	4.648	4.673	0.013	6.920	6.898	6.903	0.000
	act3B	4.641	4.639	4.660	0.052	6.885	6.867	6.923	0.008
	act3C	4.669	4.671	4.665	0.056	6.920	6.912	6.908	0.005
$Act(H_2O)_4$	act4A	4.760	4.755	4.774	0.067	7.124	7.096	7.084	0.007
	act4B	4.691	4.697	4.707	0.039	7.038	7.029	7.045	0.004
	act4C	4.676	4.672	4.696	0.069	6.973	6.950	7.016	0.009
$Act(H_2O)_5$	act5A	4.780	4.765	4.753	0.052	6.938	6.892	6.909	0.010
	act5B	4.752	4.749	4.764	0.067	7.126	7.091	7.119	0.010
	act5C	4.733	4.726	4.746	0.067	7.089	7.051	7.055	0.008

[a]Eq. (3).
[b]One-body vertical transition energy, defined as $E^*_M - E^0_M$.
[c]Two-body part of the solvent polarization, defined as $\sum_{I \neq M} (P_{IJ} - P_I - P_J)$.

Table III: Excitation energies (in eV) for acrolein-water clusters together with a decomposition of the many-body contributions. The geometries have been optimized at the DF-LMP2/cc-pVTZ level, the excitation energies have been computed with EOM-CCSD/aug-cc-pVDZ.

		$n \rightarrow \pi^*$				$\pi \rightarrow \pi^*$			
Structure	Tag	FULL	R2B-VTE[a]	1B-VTE[b]	2B-Pol[c]	FULL	R2B-VTE[a]	1B-VTE[b]	2B-Pol[c]
Acr		3.880				6.845			
$Acr(H_2O)_1$	acr1A	4.047	4.047	4.042	—	6.835	6.835	6.865	—
	acr1B	3.916	3.916	3.917	—	6.809	6.809	7.210	—
	acr1C	4.051	4.051	4.064	—	6.754	6.754	6.774	—
$Acr(H_2O)_2$	acr2A	4.074	4.076	4.060	0.000	6.806	6.806	6.856	0.004
	acr2B	4.052	4.051	4.071	0.000	6.793	6.795	6.833	0.000
	acr2C	4.077	4.078	4.078	0.000	6.783	6.782	6.816	0.000
$Acr(H_2O)_3$	acr3A	4.051	4.051	4.080	-0.005	6.740	6.744	6.775	0.002
	acr3B	4.121	4.122	4.125	0.000	6.691	6.691	6.730	0.000
	acr3C	4.090	4.093	4.096	0.000	6.746	6.745	6.790	-0.001
$Acr(H_2O)_4$	acr4A	4.178	4.172	4.141	0.001	6.658	6.665	6.758	0.008
	acr4B	4.129	4.131	4.137	0.000	6.667	6.666	6.714	-0.001
	acr4C	4.140	4.137	4.175	-0.007	6.625	6.632	6.688	0.007
$Acr(H_2O)_5$	acr5A	4.184	4.168	4.200	0.001	6.610	6.622	6.687	0.009
	acr5B	4.173	4.168	4.176	0.000	6.663	6.667	6.703	0.006
	acr5C	4.144	4.146	4.166	-0.007	6.550	6.555	6.632	0.005

[a]Eq. (3).
[b]One-body vertical transition energy, defined as $E^*_M - E^0_M$.
[c]Two-body part of the solvent polarization, defined as $\sum_{I \neq M} (P_{IJ} - P_I - P_J)$.

Table IV: Solvatochromic shifts (in eV) for the molecules under study. The computed values are obtained at the EOM-CCSD/aug-cc-pVDZ level. The $n \rightarrow 3s$ values have been left out since no converged estimate is available.

Acetone

	$n \rightarrow \pi^*$
R1B-VTE($n_w = 0$)	0.144 ± 0.017
R2B-VTE($n_w = 50$)	0.115 ± 0.015
Experiment	0.19-0.21[a]

Acrolein

	$n \rightarrow \pi^*$	$\pi \rightarrow \pi^*$
R1B-VTE($n_w = 0$)	0.286 ± 0.025	-0.269 ± 0.029
R2B-VTE($n_w = 50$)	0.240 ± 0.022	-0.558 ± 0.032
Experiment	0.25[b]	-0.52[c]

[a] - Refs. 64–66.

[b]- Refs. 42,91.

[c] - Ref. 91.

Figure Captions

Figure 1: Cluster structures of water and acetone, optimized at the DF-LMP2/cc-pVTZ level of theory. Hydrogen bonds have been depicted by dashed lines, applying an X-Y distance cutoff of 3.0 Å, and a X-H-Y angle cutoff of 35 degrees, where X and Y are the heavy atoms involved.

Figure 2: Cluster structures of water and acrolein, optimized at the DF-LMP2/cc-pVTZ level of theory. Hydrogen bonds have been depicted by dashed lines, applying an X-Y distance cutoff of 3.0 Å, and a X-H-Y angle cutoff of 35 degrees, where X and Y are the heavy atoms involved.

Figure 3: Absolute deviations in the $n \rightarrow 3s$ excitation energies ($|\Delta\omega|$) for the acetone clusters $\mathrm{Act(H_2O)}_N$ ($N \leq 3$), as computed by the many-body expansions, relative to the full EOM-CCSD results. Two basis sets have been used, aug-cc-pVDZ and aug-cc-pVTZ.

Figure 4: Computed solvatochromic shifts (in eV) of the $n \rightarrow \pi^*$ (upper panel) and $\pi \rightarrow 3s$ (lower panel) excitations of acetone, as a function of the number of water molecules included in the expansion (n_w). The error bars are given by the statistical error (from 20 configurations) but displayed only in increments of 5. The levels of theory used were EOM-CCSD/aug-cc-pVDZ and EOM-CCSD/aug-cc-pVTZ.

Figure 5: Computed solvatochromic shifts (in eV) of the $n \rightarrow \pi^*$ (upper panel) and $\pi \rightarrow \pi^*$ (lower panel) excitations of acrolein, as a function of the number of water molecules included in the expansion (n_w). The error bars are given by the statistical error (from 20 configurations) but displayed only in increments of 5. The level of theory used was EOM-CCSD/aug-cc-pVDZ.

Figures

Figure 1: Mata, Molecular Physics

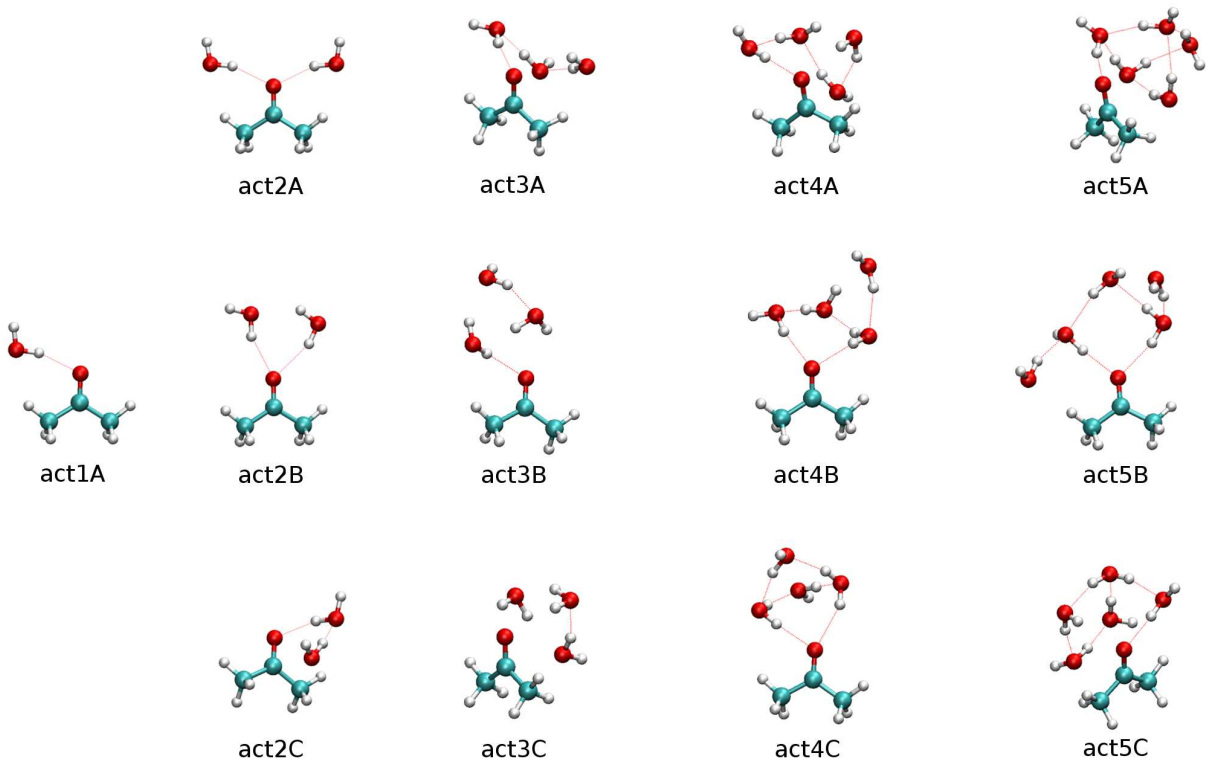

Figure 2: Mata, Molecular Physics

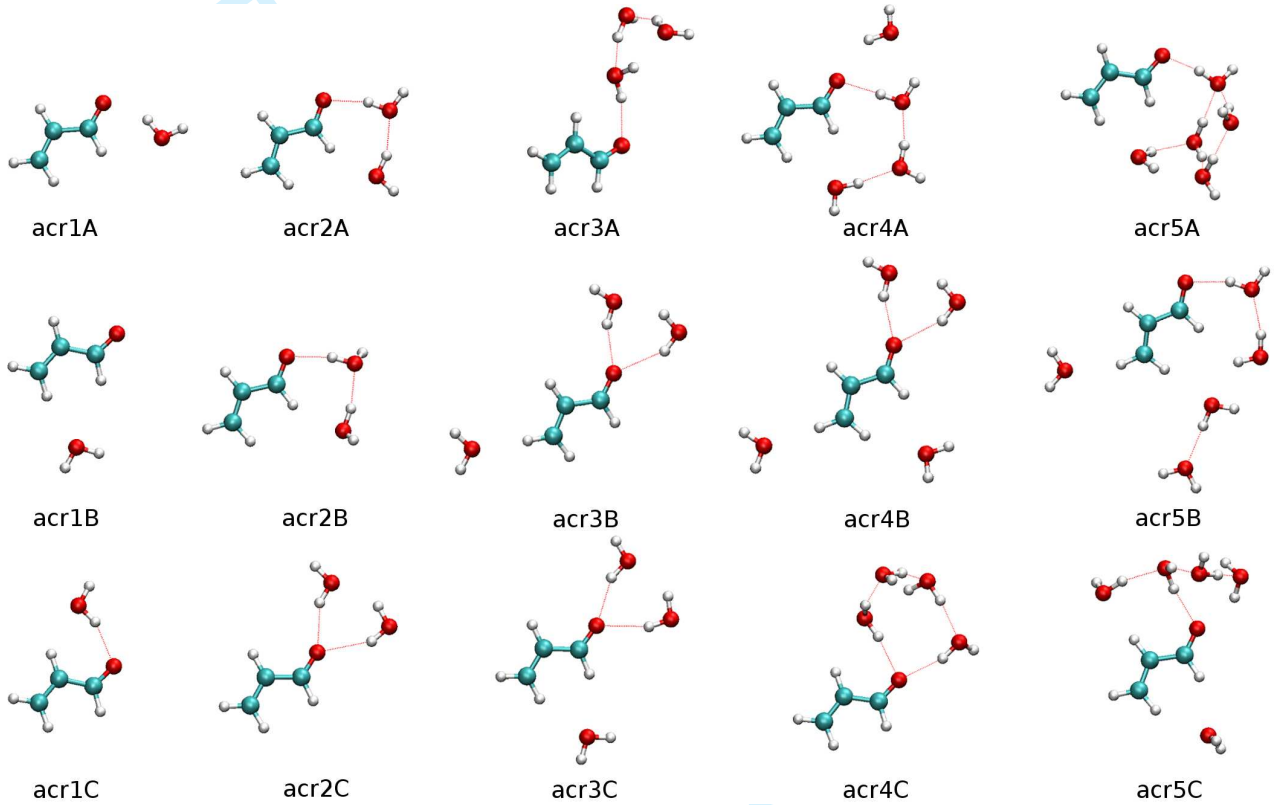

Figure 3: Mata, Molecular Physics

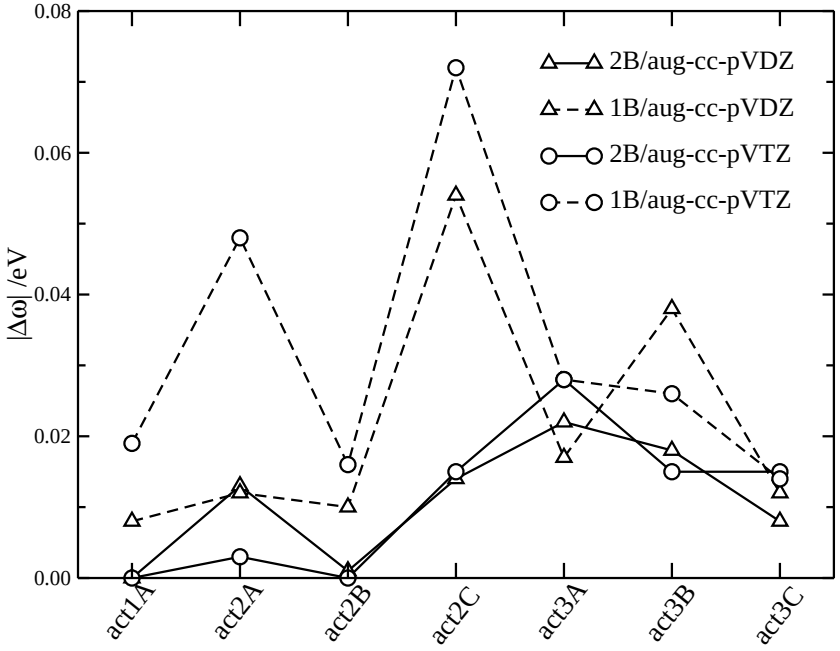

Figure 4: Mata, Molecular Physics

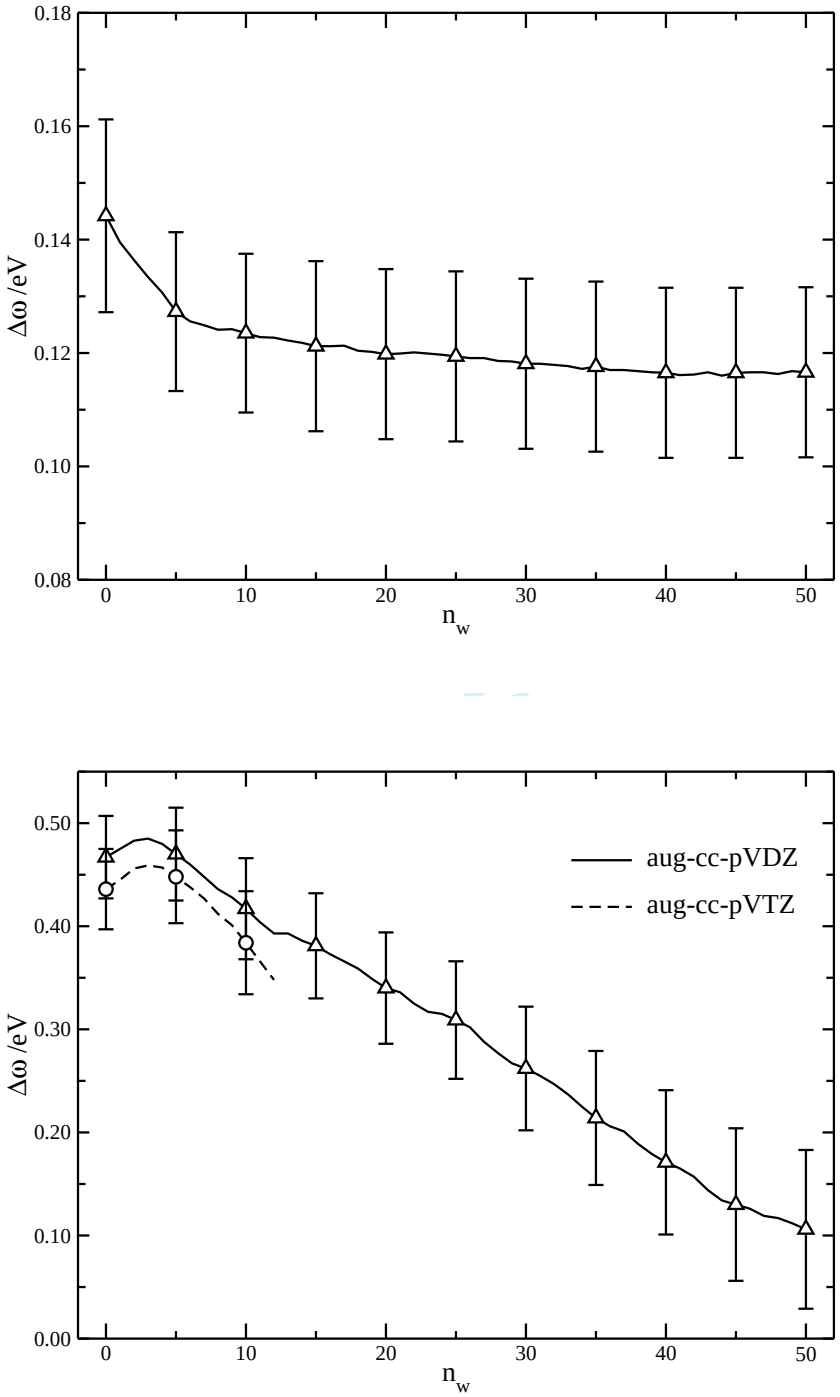

Figure 5: Mata, Molecular Physics

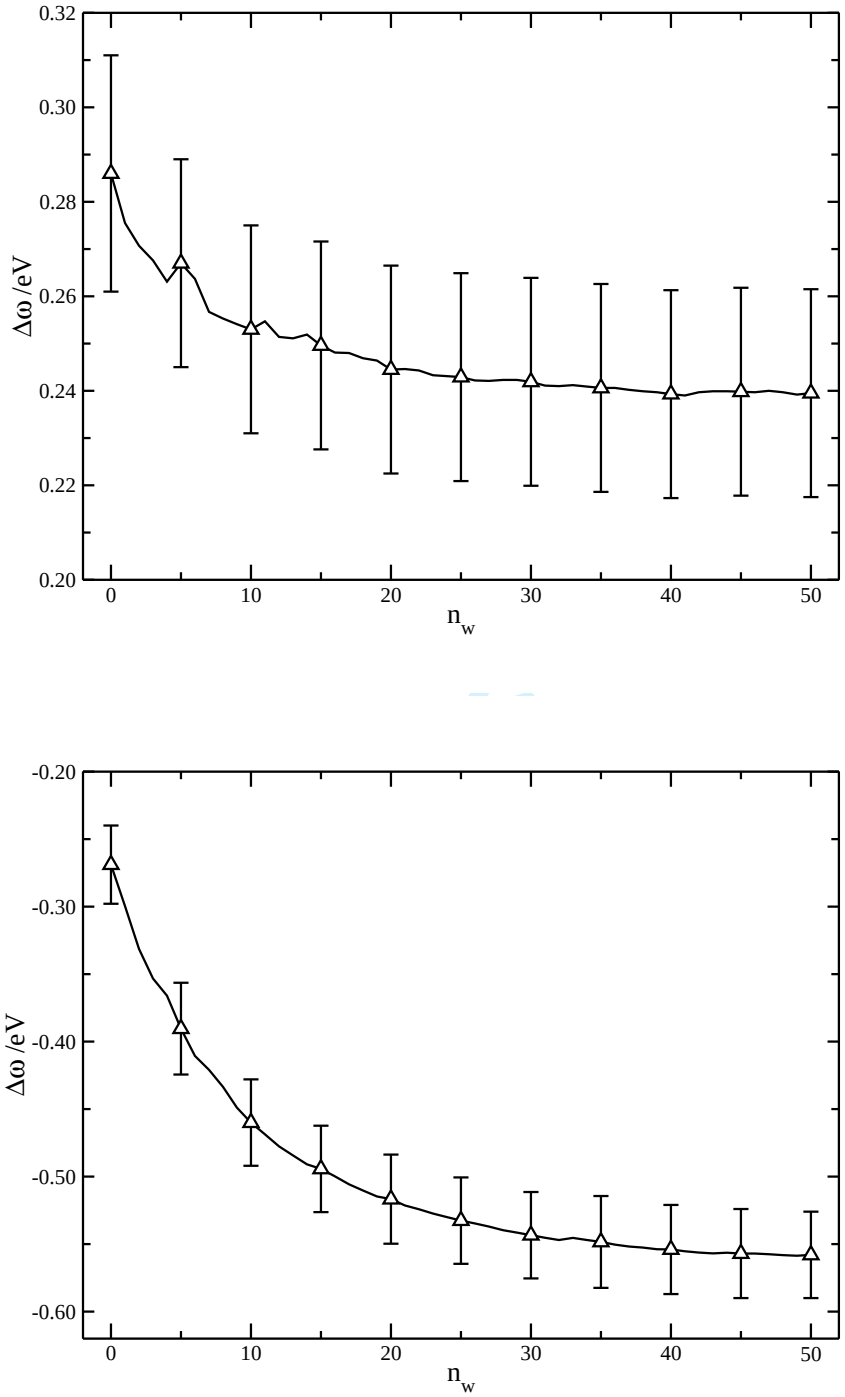

The following data includes several geometries used in the work, namely the MP2/aug-cc-pVTZ and MP2(PCM)/aug-cc-pVTZ optimized structures for acrolein and acetone, as well as the DF-LMP2/cc-pVTZ optimized monomers and clusters. All coordinates are given in Angstrom, the energies in atomic units.

```
# acetone MP2/aug-cc-pVTZ
  10
 MP2/AUG-CC-PVTZ Energy:   -192.790142749873
 C        0.0000000000      -1.2813865041      -0.6983581267
 C        0.0000000000       0.0000000000       0.0979756504
 O        0.0000000000       0.0000000000       1.3176896933
 C        0.0000000000       1.2813865041      -0.6983581267
 H        0.0000000000       2.1360571369      -0.0288646165
 H        0.8772910684       1.3152833639      -1.3455373070
 H       -0.8772910684       1.3152833639      -1.3455373070
 H        0.0000000000      -2.1360571369      -0.0288646165
 H       -0.8772910684      -1.3152833639      -1.3455373070
 H        0.8772910684      -1.3152833639      -1.3455373070

# acrolein MP2/aug-cc-pVTZ
   8
 MP2/AUG-CC-PVTZ Energy:   -191.555490552926
 C       -0.3630331264       0.0000000000       0.5887250652
 O        0.1016143365       0.0000000000       1.7156021446
 C        0.4451173518       0.0000000000      -0.6384946939
 C       -0.1535159509       0.0000000000      -1.8357034990
 H       -1.4570715901       0.0000000000       0.4247660286
 H        1.5212352678       0.0000000000      -0.5250806049
 H        0.4085233992       0.0000000000      -2.7581900009
 H       -1.2344407129       0.0000000000      -1.9058536343

# acetone MP2(PCM)/aug-cc-pVTZ
  10
 MP2(PCM)/AUG-CC-PVTZ Energy: -192.7970426
C        0.000000    1.277453   -0.613375
C        0.000000    0.000000    0.178992
O        0.000000    0.000000    1.404189
C        0.000000   -1.277453   -0.613375
H        0.000000   -2.137952    0.049185
H       -0.877369   -1.303726   -1.261333
H        0.877369   -1.303726   -1.261333
H        0.000000    2.137952    0.049185
H        0.877369    1.303726   -1.261333
H       -0.877369    1.303726   -1.261333

# acrolein MP2(PCM)/aug-cc-pVTZ
   8
 MP2(PCM)/AUG-CC-PVTZ Energy: -191.5643348
C       -0.364488    0.000000    0.579757
O        0.097485    0.000000    1.715167
C        0.450395    0.000000   -0.636162
C       -0.155256    0.000000   -1.831630
H       -1.458825    0.000000    0.417805
H        1.531161    0.000000   -0.526659
H        0.406125    0.000000   -2.756648
```

```
H        -1.238169    0.000000   -1.895858

# acetone DF-LMP2/cc-pVTZ
  10
DF-LMP2/CC-PVTZ Energy:   -192.767062093410
C        0.6991711272        0.0000000000       -1.2850211939
C       -0.1007082240        0.0000000000        0.0000180069
C        0.6998950569        0.0000000000        1.2846065822
O       -1.3185790534        0.0000000000        0.0003583118
H        0.0289647945        0.0000000000        2.1381463650
H        1.3465268888       -0.8773209460        1.3211633512
H        1.3465268883        0.8773209460        1.3211633514
H        0.0277577514        0.0000000000       -2.1381814421
H        1.3457829720        0.8773209460       -1.3219456878
H        1.3457829717       -0.8773209460       -1.3219456878

# act1A DF-LMP2/cc-pVTZ
  13
DF-LMP2/CC-PVTZ Energy:   -269.094092045633
C        0.8320301543        0.0000000000       -1.3326401620
C       -0.0693595767        0.0000000000       -0.1200176059
O       -1.2861171780        0.0000000000       -0.2392882130
C        0.6124776791        0.0000000000        1.2271371941
H       -0.1160374536        0.0000000000        2.0315276915
H        1.2566787428       -0.8762693462        1.3074910946
H        1.2566787420        0.8762693462        1.3074910944
H        0.2365108988        0.0000000000       -2.2402769171
H        1.4794670499        0.8770306078       -1.3123008307
H        1.4794670491       -0.8770306078       -1.3123008318
O       -2.5111637018        0.0000000000        2.3968938522
H       -2.3046864047        0.0000000000        1.4511564098
H       -3.4693470014        0.0000000000        2.4300812237

# act2A DF-LMP2/cc-pVTZ
  16
DF-LMP2/CC-PVTZ Energy:   -345.420131987947
C        0.6316335272        0.0000000000       -1.2872861937
C       -0.1550113406        0.0000000000       -0.0011871151
O       -1.3820783288        0.0000000000        0.0025259324
C        0.6394038468        0.0000000000        1.2801286096
H       -0.0135418280        0.0000000000        2.1467044976
H        1.2884870508       -0.8759209830        1.3008644431
H        1.2884870503        0.8759209830        1.3008644438
H       -0.0265680824        0.0000000000       -2.1498771925
H        1.2805730746        0.8759269074       -1.3119402550
H        1.2805730738       -0.8759269074       -1.3119402564
O       -2.3335304133        0.0000000000        2.7777391839
H       -2.2497037599        0.0000000000        1.8145336391
H       -3.2793173612        0.0000000000        2.9353160866
O       -2.3489747953        0.0000000000       -2.7680974340
H       -2.2580722102        0.0000000000       -1.8055242941
H       -3.2959005039        0.0000000000       -2.9187400951

# act2B DF-LMP2/cc-pVTZ
  16
DF-LMP2/CC-PVTZ Energy:   -345.418110132412
```

C	0.7478398631	0.0000000000	-1.2845521418
C	0.1531830780	0.0000000000	0.1015090427
O	-1.0560308235	0.0000000000	0.2797664435
C	1.1240163320	0.0000000000	1.2568788365
H	0.5873737013	0.0000000000	2.2004680885
H	1.7688235584	-0.8770571997	1.1970412715
H	1.7688235598	0.8770571997	1.1970412714
H	-0.0372343699	0.0000000000	-2.0342492271
H	1.3828051481	0.8770345158	-1.4125241668
H	1.3828051466	-0.8770345158	-1.4125241686
O	-3.6958268399	0.0000000000	1.6142039878
H	-2.7420053866	0.0000000000	1.4731608760
H	-3.8023654312	0.0000000000	2.5667666457
O	-3.6768834229	0.0000000000	-1.3899502834
H	-2.7608786222	0.0000000000	-1.0964279545
H	-4.1455074911	0.0000000000	-0.5487315214

act2C DF-LMP2/cc-pVTZ
16
DF-LMP2/CC-PVTZ Energy: -345.424997283824

C	0.7008880971	0.3341886708	-1.2938822264
C	-0.0300575857	0.6346665004	-0.0104406361
O	-0.7659037054	1.6082751877	0.0861877731
C	0.1801071356	-0.3349971558	1.1242446794
H	-0.4432966113	-0.0739607727	1.9739539013
H	-0.0626992957	-1.3408053115	0.7847777899
H	1.2304439393	-0.3224038305	1.4181719501
H	0.6338460561	1.1802566229	-1.9710648483
H	1.7420390803	0.0777978014	-1.1033030313
H	0.2215334470	-0.5352245086	-1.7458087089
O	-3.0421664239	0.6480192059	1.4335382949
H	-2.3207711064	1.2074956419	1.1001257208
H	-3.8023041687	1.2314281572	1.4826432674
O	-2.3638863631	-1.3866553184	-0.5069879835
H	-2.9852430629	-1.3674038257	-1.2377427204
H	-2.7575414813	-0.7850050081	0.1445849049

act3A DF-LMP2/cc-pVTZ
19
DF-LMP2/CC-PVTZ Energy: -421.754574040250

C	0.1103829478	0.1957483682	-1.2439844961
C	-0.4534051312	0.3994705006	0.1405838166
C	-0.1691528659	-0.6651666348	1.1665323106
O	-1.1213749544	1.3928651737	0.4036222675
O	-3.2590369443	0.9243552373	2.1714801634
O	-3.1956187907	0.6760622698	-1.9100419725
H	-0.4684198997	-0.3393998367	2.1580570787
H	-0.7408417890	-1.5531041874	0.8920773542
H	0.8877115043	-0.9297658153	1.1551537973
H	-0.6571047775	0.4372090699	-1.9751745194
H	0.9494556420	0.8800845314	-1.3771943026
H	0.4637224681	-0.8213246328	-1.3925214192
H	-2.4615418067	1.2673576320	1.7335917249
H	-3.0720934485	0.9847253926	3.1105289268
H	-2.8883924404	1.4354415140	-1.4068014498
H	-3.3084781924	0.0030195737	-1.2228892566

```
O      -3.3913450756    -1.2197986119     0.3558953285
H      -3.4879804320    -0.5875187198     1.0891931563
H      -4.2198660137    -1.7045888246     0.3446564916

# act3B DF-LMP2/cc-pVTZ
  19
DF-LMP2/CC-PVTZ Energy:   -421.753742698064
C       1.4135716004     0.2929406634    -1.3905841039
C       0.5590244278     0.0010192514    -0.1819938204
C       1.0048171055     0.6061378969     1.1263545706
O      -0.4419847264    -0.6981312460    -0.2658025812
O      -2.2712317567    -0.2901979620     1.9745335619
O      -3.5920759246    -0.1189164836    -0.6140039752
H       0.2250889494     0.5238557247     1.8775762535
H       1.8968654705     0.0782902415     1.4682728741
H       1.2843811147     1.6496399940     0.9863567354
H       1.0810335059    -0.2976094713    -2.2385744878
H       1.3399481517     1.3542634015    -1.6318348294
H       2.4610470871     0.0857000064    -1.1725440367
H      -1.6353639298    -0.6906797479     1.3659975497
H      -2.9388154344    -0.9838258179     2.0842695810
H      -2.8100194745    -0.4099453642    -1.0931699419
H      -3.2145761541     0.1842521087     0.2272519290
O      -4.4337898498    -2.1022994049     1.2936232874
H      -4.3903185818    -3.0189467501     1.0144690166
H      -4.3472585810    -1.5921220407     0.4722014172

# act3C DF-LMP2/cc-pVTZ
  19
DF-LMP2/CC-PVTZ Energy:   -421.758206345916
C       1.0020061745     0.0933895257    -1.1432355841
C       0.1487799337     0.5754386556     0.0022425581
C       0.6762756698     0.3168512589     1.3900854465
O      -0.9309952548     1.1200592386    -0.1884559844
O      -3.0693633568    -0.1786529822     1.4439765258
O      -3.0250570417    -0.6945135352    -1.4304288603
H      -0.0042332947     0.7131722912     2.1377164528
H       0.7844967251    -0.7593179866     1.5248026319
H       1.6611892040     0.7686330163     1.5074858300
H       0.6141390377     0.4670818593    -2.0862784071
H       2.0384184192     0.4018794122    -1.0132063615
H       0.9753727148    -0.9969140785    -1.1435782265
H      -2.4716516818     0.5399783974     1.2016290314
H      -2.4882944658    -0.9498402914     1.3925706844
H      -2.4640174029     0.0739206160    -1.5872608841
H      -3.4220688441    -0.4771414218    -0.5719990566
O      -1.2476298623    -2.1863430974     0.1603742950
H      -1.3652694120    -3.1380279460     0.1138502119
H      -1.8239952620    -1.8351109321    -0.5450363034

# act4A DF-LMP2/cc-pVTZ
  22
DF-LMP2/CC-PVTZ Energy:   -498.092301264058
C      -0.1475008414    -0.5631460639    -1.5476711099
C      -0.1033775954     0.3208882678    -0.3308230147
O      -0.5434999967     1.4667036724    -0.3610572678
```

C	0.4730646756	-0.2770759101	0.9239177448
O	-3.5866347778	1.1481650604	1.7791891903
O	-2.7870714482	-1.1285460812	0.4475509350
O	-3.4562075760	1.2645039516	-1.1773136326
H	0.5655017784	0.4722903209	1.7039880385
H	-0.2063354594	-1.0636022663	1.2540115817
H	1.4394392649	-0.7354751952	0.7181647752
H	-0.5662358457	-0.0260332713	-2.3932410451
H	0.8551411072	-0.9158686610	-1.7885634459
H	-0.7625195124	-1.4328164191	-1.3188100426
H	-3.7654395846	1.5054925762	0.8971060984
H	-2.8253726308	1.6688767666	2.0819966894
H	-2.5481268531	1.5850470357	-1.2257818665
H	-3.3330197134	0.3358313089	-0.9345812591
H	-3.0580146036	-0.4344309049	1.0852280674
H	-3.3747893824	-1.8642426179	0.6349202637
O	-1.1113754617	2.5510679459	2.1961164014
H	-0.8211170662	2.3492188482	1.2903090237
H	-1.0647624774	3.5073506362	2.2637188745

act4B DF-LMP2/cc-pVTZ
22
DF-LMP2/CC-PVTZ Energy: -498.085188629318

C	0.0375386910	0.0064071380	-1.3012372694
C	-0.3484768870	0.3220151336	0.1202676015
O	-1.4053710889	0.8798166625	0.3899683231
C	0.6290957031	-0.0714065285	1.1980430660
O	-3.6295217202	0.4609780906	2.2169927864
O	-4.7905650438	-1.3374438045	0.2311307381
O	-3.4758310609	0.3053732039	-1.6880091116
H	0.3376869038	0.3556285109	2.1527496284
H	0.6488354247	-1.1595811246	1.2748725057
H	1.6358464718	0.2496383644	0.9326266454
H	-0.8319106395	0.0430200359	-1.9504159160
H	0.7695537053	0.7461185427	-1.6306551567
H	0.5157037142	-0.9698136462	-1.3613134293
H	-2.7993018428	0.7204859137	1.7948899568
H	-3.3835923485	0.2304739358	3.1154797726
H	-2.8760101457	0.7754447462	-1.0958905142
H	-3.7694248691	-0.4388596359	-1.1307994476
H	-4.4745523029	-0.8448325930	1.0028050541
H	-5.5483107795	-0.8116327814	-0.0648089494
O	-6.2679847432	0.8156239250	-1.1180275939
H	-5.3713305043	0.8780787821	-1.4852257224
H	-6.3381416376	1.5893621287	-0.5538569678

act4C DF-LMP2/cc-pVTZ
22
DF-LMP2/CC-PVTZ Energy: -498.089946634126

C	1.4358696581	-0.0863614286	-1.3703859575
C	0.6301480537	0.1897195852	-0.1261017698
O	-0.5684925047	0.4314530784	-0.1837370833
C	1.3697342079	0.1594103317	1.1879733189
O	-2.1782845356	0.4366168792	2.2897722063
O	-3.4878206513	-0.1404539902	-0.9840148035
O	-3.4130726375	-1.8716491724	1.2261476932

H	0.6757040562	0.2183004249	2.0212640557
H	1.9714580913	-0.7460957585	1.2613616876
H	2.0582281810	1.0051615857	1.2256467457
H	0.8279328372	0.0690677669	-2.2561838670
H	2.3160941000	0.5559213584	-1.3994144421
H	1.7920475720	-1.1172312994	-1.3459894118
H	-1.6134921346	0.5154271002	1.5077941280
H	-2.5509225130	-0.4544999142	2.1776365578
H	-2.5583315866	0.1040642691	-1.0528223585
H	-3.8709911778	0.5965932521	-0.4756204686
H	-3.2713209021	-2.7927950848	1.0021132437
H	-3.5113554165	-1.4126694583	0.3704299836
O	-4.2930268021	1.7551383091	0.9616470254
H	-3.6261932221	1.4084817248	1.5837052209
H	-4.1747746734	2.7068554408	0.9844592953

act5A DF-LMP2/cc-pVTZ
25
DF-LMP2/CC-PVTZ Energy: -574.423711752946

C	0.0597917928	0.8906760603	-1.2338919722
C	-0.6029548167	0.6929947826	0.1016726750
C	-0.6551038814	-0.7172643328	0.6257743373
O	-1.0683517520	1.6425821100	0.7225260044
O	-3.3391545909	1.4559795858	2.2298734880
O	-4.1510026457	-1.1792034891	1.1329687241
O	-3.2248610566	-0.0450714903	-1.3714772043
O	-6.3671542673	-0.2573298084	-0.4972829766
H	-1.3150766327	-0.7944282413	1.4838913540
H	-0.9894134486	-1.3933304746	-0.1584814173
H	0.3547479540	-1.0156258732	0.9138096055
H	0.2435418912	1.9458550106	-1.4120318251
H	0.9871026004	0.3230086887	-1.2981850245
H	-0.6251972591	0.5034701477	-1.9895217307
H	-2.4403578607	1.5207908762	1.8449440942
H	-3.2653693438	1.8098059701	3.1192041360
H	-3.5947815144	0.8241567673	-1.1734253610
H	-3.4357940156	-0.5404659779	-0.5620876659
H	-3.9961706796	-0.4148108803	1.7028640946
H	-5.0447265503	-1.0276687186	0.7855977886
H	-5.8777129025	-0.5212490109	-1.2835510384
H	-6.0701203193	0.6553854218	-0.3679605121
O	-4.8304698406	2.1681180040	-0.0475980795
H	-4.9475756795	3.1094947960	-0.1919853897
H	-4.3880191811	2.0945210764	0.8159208958

act5B DF-LMP2/cc-pVTZ
25
DF-LMP2/CC-PVTZ Energy: -574.413988252103

C	0.1891484356	-0.4194855924	-1.6561310242
C	-0.3042432091	0.0773647941	-0.3228466574
C	0.7007410627	0.7317203162	0.5849066296
O	-1.4790258100	-0.0615562538	0.0039061052
O	-2.9943955197	0.6495066079	2.3117432029
O	-5.5396078527	-0.1828161009	0.9371705456
O	-3.9910917761	-0.9678840425	-1.3641959847
O	-5.7835845821	1.2276968348	-1.5860953975

H	0.2160732511	1.3439053046	1.3411418098
H	1.2739903055	-0.0582927484	1.0753743620
H	1.4076826885	1.3255646807	0.0077754546
H	-0.5691087981	-1.0215790844	-2.1475299954
H	0.4364025466	0.4396152412	-2.2816731830
H	1.1059659314	-0.9940573394	-1.5270769252
H	-2.4398621782	0.3764358497	1.5596325143
H	-2.9554825181	-0.0954136753	2.9187420583
H	-3.1115209204	-0.7222724948	-1.0526266318
H	-4.5035510938	-1.0079832336	-0.5389211707
H	-4.8537643617	0.2758321216	1.4388971141
H	-5.8343056032	0.4756068431	0.2905206908
H	-5.1057733233	0.5561504823	-1.7759649875
H	-5.3873693899	2.0558262221	-1.8633325727
O	-0.9413890568	2.5723508728	2.9896206195
H	-1.2458178098	3.4805401105	3.0419329475
H	-1.7546564185	2.0556932842	2.8928464755

act5C DF-LMP2/cc-pVTZ
25
DF-LMP2/CC-PVTZ Energy: -574.426872561210

C	0.4262394721	0.2257838623	-0.9440726933
C	0.5725401082	0.4907058706	0.5311492618
C	1.2842436813	-0.5577559056	1.3419258647
O	0.1146623209	1.4995425338	1.0588381294
O	-2.3623171308	0.5559847024	2.6196258766
O	-1.8575414357	-1.6558048024	0.8212790689
O	-3.5808788107	-0.5563841288	-0.9835713641
O	-3.9143857239	1.7249351853	0.4751958196
H	1.4625962690	-0.1989582766	2.3510188706
H	0.6477000902	-1.4423447324	1.3694107020
H	2.2240277012	-0.8369587686	0.8671749472
H	-0.1424874331	1.0163341706	-1.4240525039
H	1.4132197242	0.1469102181	-1.4005592144
H	-0.0742706593	-0.7329024176	-1.0763593683
H	-1.5239754131	1.0275047666	2.5786416130
H	-2.1793349899	-0.2556890887	2.1174504470
H	-3.3623334012	-0.2949602649	-1.8801915139
H	-3.7928709083	0.2880482663	-0.5231537300
H	-2.2470897693	-2.4916666797	1.0900059036
H	-2.4522785267	-1.3342326904	0.1087675791
H	-3.5249788249	1.4254002799	1.3142029417
H	-3.2379263372	2.3229092447	0.1205278569
O	-1.5972730060	3.0957300941	-0.5480787595
H	-0.9470104652	2.6664015185	0.0345172776
H	-1.4295585323	4.0358720428	-0.4515850120

acrolein DF-LMP2/cc-pVTZ
8
DF-LMP2/CC-PVTZ Energy: -191.534474076489

C	-0.3634559001	0.0000000000	0.5939366085
O	0.1020758207	0.0000000000	1.7182361672
C	0.4444594062	0.0000000000	-0.6392950199
C	-0.1531734816	0.0000000000	-1.8371715452
H	-1.4582459517	0.0000000000	0.4273266946
H	1.5211176187	0.0000000000	-0.5274491096

```
H        0.4096928385      0.0000000000      -2.7594850779
H       -1.2340413757      0.0000000000      -1.9103279123

# acr1A DF-LMP2/cc-pVTZ
  11
DF-LMP2/CC-PVTZ Energy:   -267.860487301409
C        1.0022944540      0.0000000000      -2.1343839998
C        1.3025530760      0.0000000000      -0.8293054340
C        0.2248879723      0.0000000000       0.1706422120
O        0.4187858581      0.0000000000       1.3774847378
H       -0.8021875743      0.0000000000      -0.2326371518
H        2.3219491803      0.0000000000      -0.4660630089
H        1.7664657012      0.0000000000      -2.8982595363
H       -0.0311882032      0.0000000000      -2.4584431193
H       -1.4903696706      0.0000000000       1.9948500484
O       -2.4342357118      0.0000000000       1.7850963256
H       -2.8646830820      0.0000000000       2.6415519262

# acr1B DF-LMP2/cc-pVTZ
  11
DF-LMP2/CC-PVTZ Energy:   -267.855972387096
C        1.7756140871      0.0000000000      -1.8414006306
C        1.4212299586      0.0000000000      -0.5494322120
C       -0.0050094937      0.0000000000      -0.1811115746
O       -0.4205249976      0.0000000000       0.9641364436
O       -1.0277384619      0.0000000000      -3.9595500552
H       -0.6975142218      0.0000000000      -1.0435743862
H        2.1439756450      0.0000000000       0.2567464621
H        2.8135937424      0.0000000000      -2.1438519406
H        1.0176168801      0.0000000000      -2.6155015639
H       -0.9941359443      0.0000000000      -4.9195105784
H       -1.9687781939      0.0000000000      -3.7662339642

# acr1C DF-LMP2/cc-pVTZ
  11
DF-LMP2/CC-PVTZ Energy:   -267.861594350178
C        0.8508542035      0.0000000000      -2.2922991862
C        1.2571052087      0.0000000000      -1.0156814057
C        0.2515110728      0.0000000000       0.0571758548
O        0.5059929721      0.0000000000       1.2520473102
O        3.4233170131      0.0000000000       1.3706215841
H       -0.7988317885      0.0000000000      -0.2873146489
H        2.3011275426      0.0000000000      -0.7309631359
H        1.5520076055      0.0000000000      -3.1144011669
H       -0.2051157685      0.0000000000      -2.5349833235
H        2.4835065780      0.0000000000       1.5994790366
H        3.8750123607      0.0000000000       2.2164040813

# acr2A DF-LMP2/cc-pVTZ
  14
DF-LMP2/CC-PVTZ Energy:   -344.190880472019
C        0.4493486189      0.0000000000      -2.0551796486
C        0.8686617966      0.0000000000      -0.7828066365
C       -0.1201863073      0.0000000000       0.3036500224
O        0.1851387442      0.0000000000       1.4910691809
H       -1.1745347969      0.0000000000      -0.0120064402
```

```
H        1.9166166937      0.0000000000      -0.5124290296
H        1.1403317764      0.0000000000      -2.8860035407
H       -0.6103584159      0.0000000000      -2.2791422669
H       -1.4269728198      0.0000000000       2.4922564020
O       -2.3723129172      0.0000000000       2.7165895032
H       -2.4064298871      0.0000000000       3.6738054954
H       -3.3369358598      0.0000000000       1.0685880814
O       -3.4780721373      0.0000000000       0.1099710505
H       -4.4313364885      0.0000000000       0.0111388268

# acr2B DF-LMP2/cc-pVTZ
  14
DF-LMP2/CC-PVTZ Energy:   -344.192567919178
C        1.0480078451      1.0262279015      -1.4449258632
C        0.9107529111     -0.2347564980      -1.0137633643
C        0.1912402537     -0.4966975179       0.2398636887
O        0.0162927588     -1.6236537413       0.6909303640
H       -0.1929840739      0.3893644556       0.7693094828
H        1.3081379729     -1.0836333602      -1.5549508816
H        1.5669659474      1.2648092485      -2.3622725519
H        0.6320396095      1.8465406847      -0.8728736698
H       -0.9785232638     -1.5257894967       2.3056877963
O       -1.5171051083     -1.2384560941       3.0632284575
H       -2.3485222566     -1.7044991870       2.9494438572
O       -1.3796263243      1.5444860016       2.4635487187
H       -0.9542365255      1.9735851347       3.2088099275
H       -1.5318677462      0.6381444683       2.7788340379

# acr2C DF-LMP2/cc-pVTZ
  14
DF-LMP2/CC-PVTZ Energy:   -344.184240038691
C        1.4817492798      0.0000000000      -2.0666407774
C        1.1780392217      0.0000000000      -0.7622862654
C       -0.2279774685      0.0000000000      -0.3373404099
O       -0.5941221202      0.0000000000       0.8274786704
H       -0.9678347310      0.0000000000      -1.1564982539
H        1.9361103965      0.0000000000       0.0100309163
H        2.5041012580      0.0000000000      -2.4159860644
H        0.6971725454      0.0000000000      -2.8133222092
H       -2.6296556889      0.0000000000       1.9038659621
O       -3.1712752989      0.0000000000       2.6977797806
H       -2.5014525712      0.0000000000       3.3900019227
O       -0.3873087864      0.0000000000       3.7856137474
H        0.4426878826      0.0000000000       4.2649231623
H       -0.1372059186      0.0000000000       2.8548288185

# acr3A DF-LMP2/cc-pVTZ
  17
DF-LMP2/CC-PVTZ Energy:   -420.522356792632
C        2.1850893000     -0.5319001025      -1.5617497221
C        1.0623999651     -0.2315361734      -0.8952201682
C       -0.1678762773      0.0488835696      -1.6489669967
O       -1.2457265050      0.3281662261      -1.1448608335
O       -0.8969504158      0.2918726938       1.7523155853
O       -2.4410654770     -0.3582616308       4.0116681263
H       -0.0675196735     -0.0080669863      -2.7480218552
```

H	1.0122711820	-0.1862613272	0.1851169040
H	3.1125774624	-0.7458830596	-1.0504156525
H	2.1905541929	-0.5677137205	-2.6446587393
H	-3.2972034376	-0.7428880457	3.8129201425
H	-1.9477030026	-0.4208530731	3.1746423641
H	-1.0096401699	1.1785134025	2.1295842877
H	-1.1970139066	0.3667760448	0.8349799163
O	-1.6643601040	2.3449981877	3.5952037300
H	-2.0804165053	1.5523641147	3.9731717768
H	-2.3883896273	2.9645818797	3.4845331345

acr3B DF-LMP2/cc-pVTZ
17
DF-LMP2/CC-PVTZ Energy: -420.506859831127

C	1.3555038490	0.0000000000	-1.9569382727
C	1.0149083636	0.0000000000	-0.6605922830
C	-0.3985185503	0.0000000000	-0.2739930003
O	-0.8014860602	0.0000000000	0.8799664722
O	-0.4378184233	0.0000000000	3.7972598449
O	-3.2811241062	0.0000000000	2.8654121828
H	-1.1151854096	0.0000000000	-1.1137857249
H	1.7527667248	0.0000000000	0.1312928034
H	2.3863748818	0.0000000000	-2.2826091253
H	0.5817986365	0.0000000000	-2.7160241243
H	-2.7891462604	0.0000000000	2.0396074617
H	-2.5708637029	0.0000000000	3.5160622091
H	0.4284084587	0.0000000000	4.2071450694
H	-0.2647104649	0.0000000000	2.8481940636
O	4.6450005148	0.0000000000	-2.8955554431
H	5.4229609496	0.0000000000	-2.3325763926
H	5.0079675993	0.0000000000	-3.7846257408

acr3C DF-LMP2/cc-pVTZ
17
DF-LMP2/CC-PVTZ Energy: -420.507370092007

C	1.8983965787	0.0000000000	-1.9422789185
C	1.5759160659	0.0000000000	-0.6413692354
C	0.1599234965	0.0000000000	-0.2560327500
O	-0.2393112966	0.0000000000	0.9002034513
O	-0.6872142254	0.0000000000	3.8363592511
O	-3.1141413491	0.0000000000	2.0571210399
H	-0.5494689689	0.0000000000	-1.0980829922
H	2.3165481086	0.0000000000	0.1478885422
H	2.9274611952	0.0000000000	-2.2727044471
H	1.1172994986	0.0000000000	-2.6925256783
H	-2.3315696795	0.0000000000	1.4971531952
H	-2.7172611427	0.0000000000	2.9343261240
H	0.0227875243	0.0000000000	4.4802968717
H	-0.2416898940	0.0000000000	2.9817526409
O	-1.2422639271	0.0000000000	-3.6163406416
H	-1.2775820565	0.0000000000	-4.5762084296
H	-2.1679919283	0.0000000000	-3.3581160236

acr4A DF-LMP2/cc-pVTZ
20
DF-LMP2/CC-PVTZ Energy: -496.848650390415

C	2.0492188686	0.0000000000	-2.1020960099
C	1.8606721463	0.0000000000	-0.7739693075
C	0.4902226348	0.0000000000	-0.2610634037
O	0.2018403258	0.0000000000	0.9321149837
O	-1.3083140268	0.0000000000	3.5567407706
O	-2.6898016135	0.0000000000	0.9477330252
O	-1.1526817141	0.0000000000	-3.3411252367
H	-0.2938879610	0.0000000000	-1.0322791182
H	2.6736652894	0.0000000000	-0.0594716694
H	3.0409648957	0.0000000000	-2.5324087389
H	1.1935623408	0.0000000000	-2.7671018947
H	-1.7215525830	0.0000000000	0.9726776524
H	-2.9177681657	0.0000000000	1.8817999229
H	-0.9547657213	0.0000000000	4.4480849282
H	-0.5295146043	0.0000000000	2.9898952531
H	-1.4073935076	0.0000000000	-4.2655842196
H	-2.0012057170	0.0000000000	-2.8661536712
O	-3.4637980822	0.0000000000	-1.7131029370
H	-4.4130604545	0.0000000000	-1.8407209294
H	-3.3370603505	0.0000000000	-0.7479944000

acr4B DF-LMP2/cc-pVTZ
20
DF-LMP2/CC-PVTZ Energy: -496.829163132426

C	1.5525078685	0.0000000000	-1.8256894194
C	1.2379207512	0.0000000000	-0.5217951525
C	-0.1715678384	0.0000000000	-0.1245442588
O	-0.5652024932	0.0000000000	1.0350375311
O	-0.4930012736	0.0000000000	3.9677547472
O	-3.2060582692	0.0000000000	2.6710393024
O	4.8641920260	0.0000000000	-2.8143740438
H	-0.8880340403	0.0000000000	-0.9606129316
H	1.9862081238	0.0000000000	0.2605511720
H	2.5780372411	0.0000000000	-2.1682471029
H	0.7573548808	0.0000000000	-2.5618912911
H	-2.5691799441	0.0000000000	1.9498097206
H	-2.6244681526	0.0000000000	3.4385292288
H	0.3302611016	0.0000000000	4.4583115700
H	-0.2268832098	0.0000000000	3.0402466033
H	5.6352957195	0.0000000000	-2.2421072097
H	5.2378817012	0.0000000000	-3.6988905269
O	-1.6943422152	0.0000000000	-3.4277390969
H	-1.7345105091	0.0000000000	-4.3873333852
H	-2.6185274682	0.0000000000	-3.1645014568

acr4C DF-LMP2/cc-pVTZ
20
DF-LMP2/CC-PVTZ Energy: -496.852872699554

C	2.2001483218	0.0857929425	-1.8079895302
C	1.3049919666	-0.0464186622	-0.8190045323
C	0.0292881861	-0.7106042386	-1.0975082837
O	-0.8533216426	-0.8820790620	-0.2662798213
O	0.0431361959	0.3276057546	2.3254594249
O	-2.5908866182	-0.3600284480	3.6476522402
O	-1.9632823200	2.2933878180	2.9598025274
H	-0.1072937125	-1.0657548915	-2.1333995108

H	1.4774908865	0.3147508550	0.1870992230
H	3.1541276827	0.5684076401	-1.6519151005
H	1.9862882714	-0.2927651026	-2.8003700963
H	-2.9457150920	-0.7771730063	2.8472978267
H	-1.6359996285	-0.4588338032	3.5345786274
H	-0.4591398676	1.1515502095	2.4357411991
H	-0.3576677647	-0.0695457724	1.5422688765
H	-2.4088956139	1.4875865279	3.2799516873
H	-2.6005324716	2.7011795698	2.3702407242
O	-3.3981928691	-1.5274753797	1.0975665168
H	-2.6554472558	-1.4103514895	0.4916780540
H	-3.5406966544	-2.4767764615	1.1154569480

acr5A DF-LMP2/cc-pVTZ
23
DF-LMP2/CC-PVTZ Energy: -573.191470650100

C	2.1163240281	0.3257917578	-2.1109687906
C	2.2420614545	0.4052516347	-0.7771489615
C	1.0999615181	0.0417134829	0.0605833563
O	1.1227089706	0.0617276969	1.2902566716
O	-3.0576715091	1.2317182452	1.0820321839
O	-3.6514907481	-0.0498278137	-1.3130913248
O	-1.0245058012	-0.8654037014	-2.5018752769
O	-1.3594475480	-0.7833928457	2.0850662836
H	0.1946599711	-0.2582072915	-0.4872715339
H	3.1532674668	0.7208686140	-0.2854764577
H	2.9354747675	0.5804401116	-2.7691569094
H	1.1808046114	-0.0028649451	-2.5492930178
H	-2.5579507996	2.0503810534	1.1168086649
H	-2.4942965578	0.5816800854	1.5382559960
H	-1.3692006818	-1.1246843978	2.9825077509
H	-0.4315014287	-0.5071863672	1.9231728134
H	-1.2085883630	-1.6059384192	-1.9044374532
H	-1.8546480215	-0.3764188884	-2.4459189806
H	-4.5746465998	0.0808169460	-1.5398904683
H	-3.5059831490	0.5037245890	-0.5225580336
O	-2.2078610241	-2.4029953852	-0.3098633465
H	-2.9037803660	-1.7866129394	-0.5784012795
H	-1.9150071905	-2.0418942226	0.5367691134

acr5B DF-LMP2/cc-pVTZ
23
DF-LMP2/CC-PVTZ Energy: -573.159082216463

C	1.3503416765	0.0000000000	-0.9155060055
C	1.9652940894	0.0000000000	0.2767612493
C	1.1630453895	0.0000000000	1.5005611331
O	1.6248667261	0.0000000000	2.6348646929
O	-0.8814692120	0.0000000000	3.9840227396
O	-2.8191738281	0.0000000000	1.7783258794
O	3.7528459564	0.0000000000	-3.4111738090
O	-2.8490538129	0.0000000000	-3.9940968181
H	0.0723472389	0.0000000000	1.3401017153
H	3.0425903243	0.0000000000	0.3816025661
H	1.9144339340	0.0000000000	-1.8380261485
H	0.2669612953	0.0000000000	-0.9677653810
H	-2.1551195347	0.0000000000	1.0847837184

H	-2.2957620385	0.0000000000	2.5912307488
H	-0.8934569261	0.0000000000	4.9421507925
H	0.0587026297	0.0000000000	3.7428976466
H	4.6452449180	0.0000000000	-3.0563355115
H	3.8878639318	0.0000000000	-4.3617250645
H	-2.2070490679	0.0000000000	-4.7075795204
H	-3.7007251179	0.0000000000	-4.4368851549
O	-2.2663253423	0.0000000000	-1.1039788826
H	-3.1361559332	0.0000000000	-0.6940831200
H	-2.4544782962	0.0000000000	-2.0510924655

acr5C DF-LMP2/cc-pVTZ
23
DF-LMP2/CC-PVTZ Energy: -573.177186887206

C	0.9452864418	-0.0173531429	-2.7465152034
C	0.8693828515	-0.1257951930	-1.4106032101
C	-0.4282144390	-0.4414017503	-0.8121543927
O	-0.6212069030	-0.5541977795	0.3960766863
O	1.1266549427	0.5262473014	2.4629128882
O	-1.9630206018	-0.0197028703	2.9760658417
O	3.4247489638	0.5133091447	0.7712813983
O	-2.3538294240	-0.4606745614	-3.7949432676
H	-1.2590071929	-0.5779619989	-1.5207095417
H	1.7272509413	0.0166070678	-0.7627382451
H	1.8792428221	0.2196453127	-3.2366630571
H	0.0652809785	-0.1611776650	-3.3617803681
H	-1.8716037986	-0.3406209188	2.0692066204
H	-1.1128441570	-0.2604172341	3.3617830554
H	0.6582666616	1.3729467295	2.5457232986
H	0.6525203674	0.0954060132	1.7357712526
H	4.0029535459	-0.1637003486	1.1289969884
H	2.7507302844	0.6235947804	1.4630482835
H	-2.8299126936	-1.1967307341	-4.1881428677
H	-2.9383720379	0.2895489696	-3.9322702371
O	-0.8792608854	2.5852678039	2.5980839348
H	-1.4680494166	1.8312924864	2.7719646651
H	-1.0437252512	3.1929145872	3.3221834776